Structural Engineering and Mechanics, Vol. 24, No. 5 (2006) 585-599
DOI: http://dx.doi.org/10.12989/sem.2006.24.5.585

Influence of bed joint orientation on interlocking grouted stabilised mud-flyash brick masonry under cyclic compressive loading

Maqsud E. Nazar†

Power Grid Corporation of India Ltd., Sector 29, Gurgaon (Haryana)-122001, India

S. N. Sinha‡

Civil Engineering Department, Indian Institute of Technology Delhi, New Delhi-110016, India

(Received April 18, 2005, Accepted June 28, 2006)

Abstract. This paper describes a series of laboratory tests carried out to evaluate the influence of bed joint orientation on interlocking grouted stabilised mud-flyash brick masonry under uniaxial cyclic compressive loading. Five cases of loading at 0^o, 22.5^o, 45^o, 67.5^o and 90^o with the bed joints were considered. The brick units and masonry system developed by Prof. S.N. Sinha were used in present investigation. Eighteen specimens of size 500 mm × 100 mm × 700 mm and twenty seven specimens of size 500 mm × 100 mm × 500 mm were tested. The envelope stress-strain curve, common point curve and stability point curve were established for all five cases of loading with respect to bed joints. A general analytical expression is proposed for these curves which fit reasonably well with the experimental data. Also, the stability point curve has been used to define the permissible stress level in the brick masonry.

Keywords: interlocking brick; grout; uniaxial; cyclic loading; envelope curve; common point; stability point; stress-strain hysteresis.

1. Introduction

Earthen building is a very ancient form of construction and in some parts of the world would be relegated to second class status. Many ancient techniques such as adobe construction are still used in many countries today. However, such unstabilised mud construction poses problems due to poor strength under damp conditions and erosion due to rain. These problems can be overcome by soil stabilisation. Stabilised mud bricks can be produced by utilising natural soil, industrial waste like flyash and a stabilising agent like cement or lime. The stabilised mud block/brick has been in use for the last four decades and is gaining popularity in various parts of the world. The primary advantages of stabilised mud brick construction are the use of local materials, simple construction methods, high thermal and acoustic insulation, low energy consumption in manufacture and an

† Senior Design Engineer, E-mail: maqsudenazar@hotmail.com
‡ Professor, Corresponding author, E-mail: snsinha@civil.iitd.ernet.in

environmentally friendly alternative to other established products.

The behaviour of stabilised soil blocks under uniaxial compressive loading for monotonic conditions has been extensively investigated by numerous researchers (Reddy 1991, Reddy and Jagdish 1995, Walker 1995, 2000, Worthing *et al.* 1992) over a long period of time. The performance of brick masonry under cyclic loading has been done in last couple of years by Naraine and Sinha (1989), Choubey and Sinha (1991), Milad and Sinha (2000) and Senthivel and Sinha (2003). However, their findings were restricted to fired clay and sand plast (calcium silicate) bricks. Steadman *et al*. (1995) have studied the influence of block geometry and grout type on the compressive strength of block masonry and Drysdale and Guo (1995) have determined the characteristic strength of interlocking dry-stacked concrete block masonry. But the behaviour of interlocking grouted brick masorny (developed by Prof. S.N. Sinha) under cyclic loading has only been studied recently by Singh and Sinha (2004a,b) for two cases of loading perpendicular and parallel to the bed joints. The behaviour of this type of interlocking brick masonry system, with specimens loaded at other bed joint orientations under cyclic loading is yet to be investigated. Other researchers such as Chen *et al.* (1978) and Macchi (1985) also reported on the cyclic behaviour of brick masonry but in connection with the seismic design of buildings with no particular emphasis into the cyclic deformation characteristics of masonry walls. Karsan and Jirsa (1969) reported that plain concrete exhibits three fundamental stress-strain curves when subjected to cyclic loading. It has also been found that brick masonry panels also possess three similar stress-strain curves under cyclic loading. The three stress-strain curves are termed as the envelope stress-strain curve, the common point stress-strain curve and the stability point stress-strain curve.

Repeated loading-unloading cycles cause accumulation of strain that eventually produce failure as strain levels grow with increasing numbers of cycles. Abrams *et al.* (1985) proposed that residual strains in a brick masonry assemblage can accumulate with the application of load cycles and this can lead to a splitting-failure of a brick unit at a compressive stress less than the failure stress under monotonically increased load. Tests on brick masonry under cyclic loading yield useful information related to the material ductility, stiffness degradation, and energy dissipation characteristics.

This paper presents the experimental evaluation of the influence of bed joint orientation on stress-strain characteristics of interlocking grouted stabilised mud-flyash brick masonry subjected to uniaxial cyclic loading. Mathematical formulations for the cyclic stress-strain curves are also proposed.

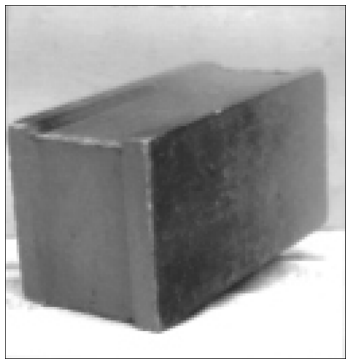

Fig. 1 Interlocking brick

Table 1 Properties of interlocking bricks and grout

Type of material	Mix proportion by weight	Water cement ratio	Mean compressive strength (N/mm^2)	Standard deviation (N/mm^2)
Interlocking stabilised mud-flyash brick	0.60 Natural soil: 0.25 Flyash : 0.15 Cement	0.50	12.12	1.41
Grout	Cement + Non-shrink material @225 gm per 50 kg of cement	0.40	38.30	4.25

2. Experimental program

2.1 Test specimen

Brick masonry panels were constructed from interlocking stabilised mud-flyash bricks of size 200 mm × 100 mm × 100 mm (Fig. 1) developed by Prof. S.N. Sinha. The square and rectangular panels that were made of these bricks measured 500 mm × 100 mm × 500 mm and 500 mm × 100 mm × 700 mm, respectively. The composition of brick units, grout and their compressive strength and standard deviation are given in Table 1, based on tests of 52 brick units and 48 mortar cubes.

Test panels were made according to the method developed by Prof. S.N. Sinha for interlocking bricks in stretcher bond pattern. Tiers of bricks were stacked with no mortar between them. Units were self aligning due to the interlocking of bricks. Cement grout poured into the joints from the top, flowed freely into the voids thereby providing adequate bond. Three grout cubes of 70 mm size used as control specimens were also cast for each test panel to determine the compressive strength of grout. Test panels were built on 20 mm thick aluminium plates and cured under damp conditions along with control specimens by covering with wet jute sacks for 28 days. All test panels were leveled and capped with gypsum plaster before testing.

2.2 Loading arrangement

A hydraulic servo-controlled compression testing machine of 4000 kN capacity was used for testing interlocking grouted brick masonry panels. Test panels were placed between the platen of the machine at the bottom and a flat compression load cell of 4000 kN range at top. Teflon sheets of 10 mm thickness were used on the two bearing surfaces of each test panel to minimise the effect of lateral platen restraint. The panels were tested under a constant rate of displacement of 0.01 mm/second and corresponding load and displacement on panel was recorded by computer through an electronic data aquisition system. The general loading arrangement and test set up are shown in Fig. 2.

2.3 Instrumentation

The interlocking stabilised mud-flyash brick masonry panels were instrumented for the measurement of axial and lateral displacements along fixed gauge lengths. Linear variable displacement transducers (LVDTs) were used on both sides of a specimen. The gauge lengths for

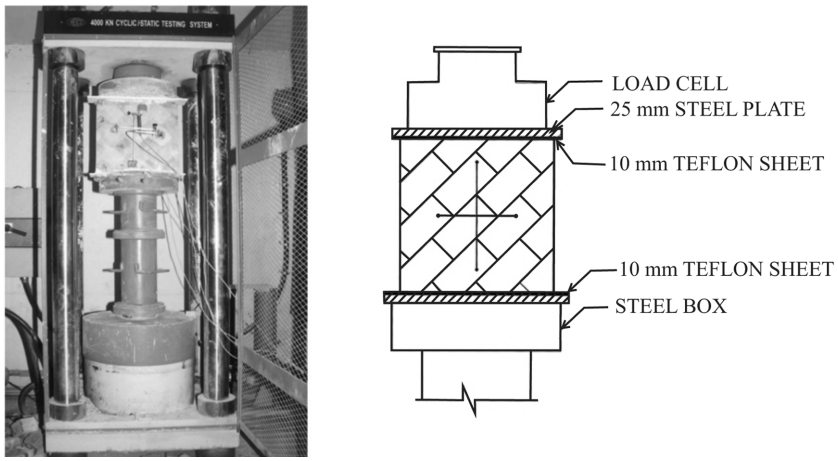

Fig. 2 Loading arrangement and test set up

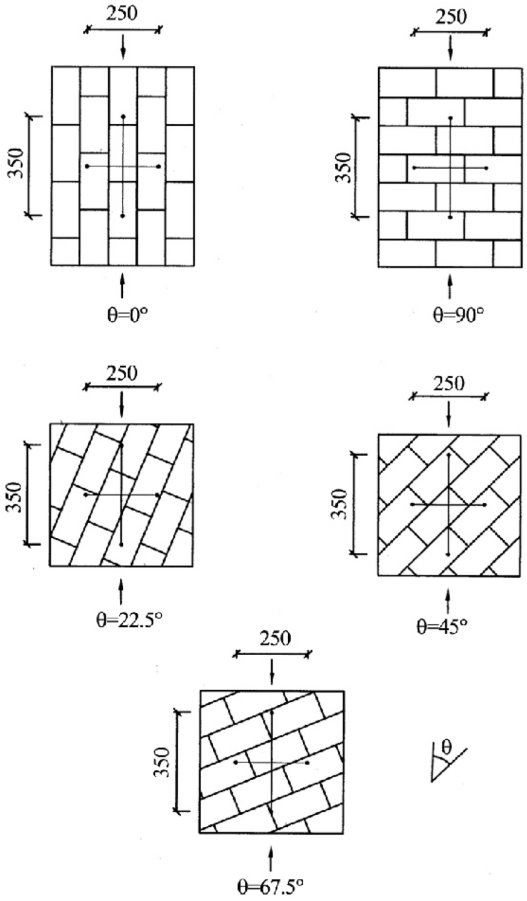

Fig. 3 Arrangement of LVDTs and loading direction

axial and lateral displacements were 350 mm and 250 mm, respectively. Preliminary trials to evaluate different positions of LVDTs and gauge length arrangements indicated that the positions of the LVDTs shown in Fig. 3 were the most appropriate. All LVDTs and load cells were connected to a data acquisition system and a computer. The displacement and load were recorded and an on-line display of load and displacement was available by monitor. The loading and unloading cycles were directly monitored and controlled by computer.

2.4 Test procedure

Three types of test as described below were conducted on 45 interlocking brick panels to investigate the influence of bed joint orientation on the behaviour of interlocking stabilised mud-flyash brick masonry in stretcher bond under uniaxial cyclic compression. Five cases of loading at 0^o, 22.5^o, 45^o, 67.5^o and 90^o with the bed joints were considered. For each load case, three panels were tested for each type of test.

Test Type I : These were monotonic uniaxial loading tests. In each case, displacement was increased uniformly upto the failure of the panel.

Test Type II : A cyclic uniaxial compressive loading tests were performed. Loading and unloading were repeated several times wherein the peak stress-strain in each cycle of loading coincided approximately with the stress-strain obtained in Type I test. The stress-strain curve so obtained possessed a locus of common points where a common point is defined as the point at which the reloading curve of any cycle cross the unloading curve of the previous cycle (e.g., point A on Fig. 4).

Test Type III : A cyclic uniaxial compressive loading test was conducted as in Test Type II except that within each cycle, loading and unloading were repeated several times. Each time unloading was done when the reloading curve intersected with the initial unloading curve until the point of intersection gradually descended and stabilised at a lower bound (e.g., point B on Fig. 5) and further cycling led to the formation of a closed hysteresis loop. Such lower bound points are termed as stability points.

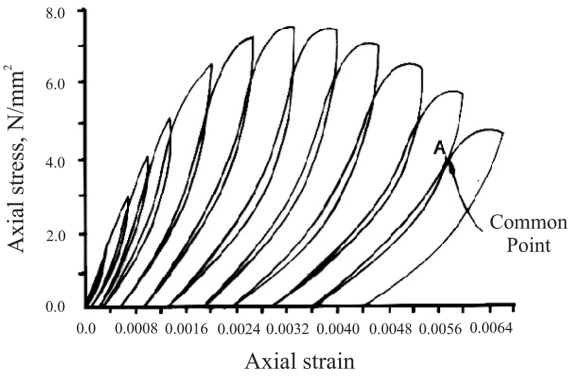

Fig. 4 Typical test under cyclic loading for common points

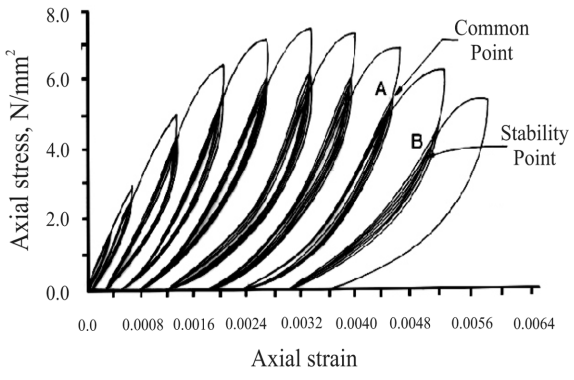

Fig. 5 Typical test under cyclic loading for stability points

3. Test results and evaluation

3.1 Failure modes

Failure and crack initiations of interlocking grouted stabilised mud-flyash brick masonry panels varied for different load cases. The panels loaded perpendicular to bed joints; displayed a typical mode of failure due to splitting of bricks through a vertical plane. Numerous micro-cracks developed parallel to the direction of the applied load. The eventual collapse of the panels was precipitated by widening of some of these micro-cracks into a few major cracks. The panels loaded at 67.5° to bed joints also showed a failure mode similar to that observed in the specimens loaded perpendicular to bed joint.

In case of panels loaded at 45° to bed joints, partial bond failures in joints were accompanied by splitting of bricks as well as central splitting at the top bearing area of a panel. The panels loaded at 22.5° to bed joints displayed a failure pattern that was confined to joints in most panels and in few panels partial, failure in bricks was also observed.

For panels loaded parallel to bed joints, cracks initiated at the bed joints. The splitting initiated at free edges and gradually propagated towards the centre of a panel. Thereafter, the separated fragments of the specimens behaved like individual compression members.

It was observed that most of the bricks were crushed partially indicating that utilization of bricks is more pronounced in interlocking grouted masonry systems. The ratio of mean compressive strength of interlocking grouted brick masonry specimens to the mean strength of bricks is given in Table 2. The ratio varies from 0.32 to 0.62 depending upon the load case. The ratio of mean compressive strength of high strength calcium silicate brick specimens (Senthivel and Sinha 2003) to the mean strength of bricks is also given in Table 2. In this case, the ratio varies from 0.05 to 0.40, depending upon the load case. It is indicated that the ultimate strength of an interlocking grouted brick masonry system is 1.55 times the ultimate strength of conventional brick masonry manufactured with high strength calcium silicate bricks for panels loaded perpendicular to bed

Table 2 Mean value of stress and strain for specimens and ratio of mean strength of specimen to mean strength of brick

Load case with respect to bed joint orientation, θ	Mean strength of panels σ_m (MPa)		Strain corresponding to peak stress, ε_m		Mean strength of panel / Mean strength of brick			
	Mean value	Standard deviation	Mean value	Standard deviation	For interlocking mud bricks (Present study)	For interlocking mud bricks (Singh and Sinha 2004a)	For calcium silicate bricks (Mulad and Sinha 2000)	For calcium silicate bricks (Senthivel and Sinha 2003)
0°	6.49	0.37	3.56×10^{-3}	1.56×10^{-4}	0.54	0.62	0.35	0.34
22.5°	3.86	0.21	0.92×10^{-3}	2.11×10^{-4}	0.32	-	-	0.05
45°	5.23	0.29	1.83×10^{-3}	1.36×10^{-4}	0.43	-	-	0.08
67.5°	5.91	0.32	3.42×10^{-3}	1.71×10^{-4}	0.49	-	-	0.32
90°	7.45	0.24	3.32×10^{-3}	1.48×10^{-4}	0.62	0.64	0.41	0.40

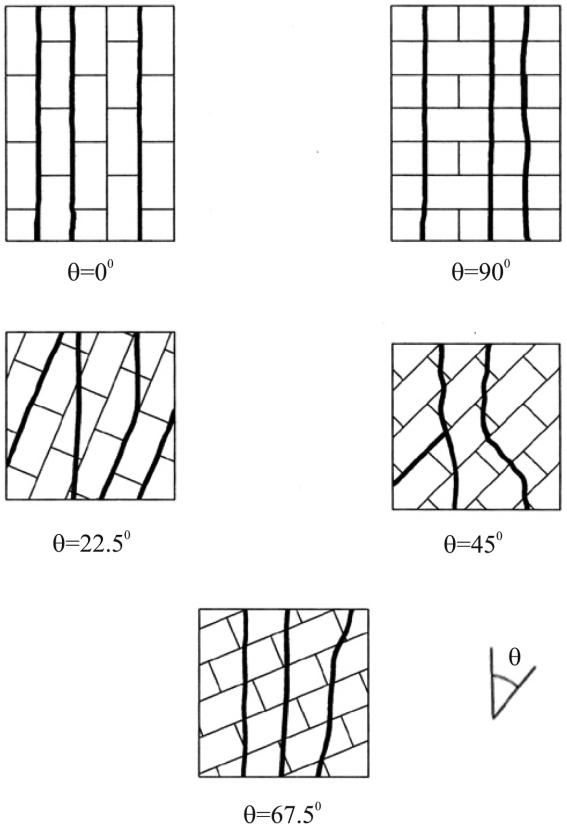

Fig. 6 Modes of failure

joints. In general, the ultimate strength of a conventional masonry system varies from 30 to 40 percent of its unit strength (Thomas 1953), but the ultimate strength of interlocking grouted brick masonry system used in this study is 62 percent for panels loaded perpendicular to bed joints.

Typical failure pattern of panels observed during experimental investigation are shown in Fig. 6.

3.2 Stress-strain curves

3.2.1 Envelope curves

The peak points of the stress-strain curve under cyclic loading (Test type II and III) were found to coincide approximately with the stress-strain curve obtained in test Type I under monotonic loading for all five load cases. Therefore, envelope point curves for all five load cases were obtained by superimposing the stress-strain curve under monotonic loading and the peak stress-strain points under cyclic loading. The envelope points obtained from test Type I, II and III have been plotted in Figs. 7 to 11 for all five case of loading. The stress coordinate has been normalised with respect to the failure (peak) stress, σ_m, of each panel and the strain coordinate has been normalised with respect to ε_m, the strain corresponding to the peak stress. The mean values of σ_m, ε_m and their standard deviations for different loading cases are given in Table 2.

The ratio of mean strength of panels loaded perpendicular to bed joints to panels loaded parallel

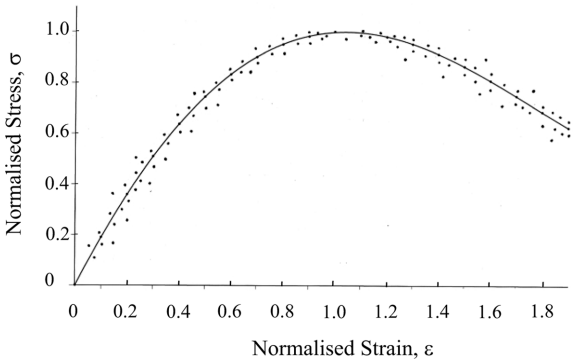

Fig. 7 Envelope stress-strain curve ($\theta = 0^{o}$)

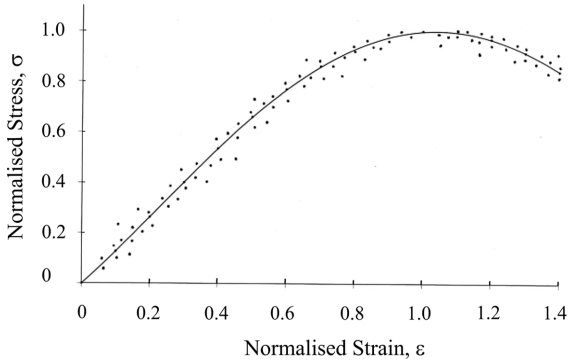

Fig. 8 Envelope stress-strain curve ($\theta = 22.5^{o}$)

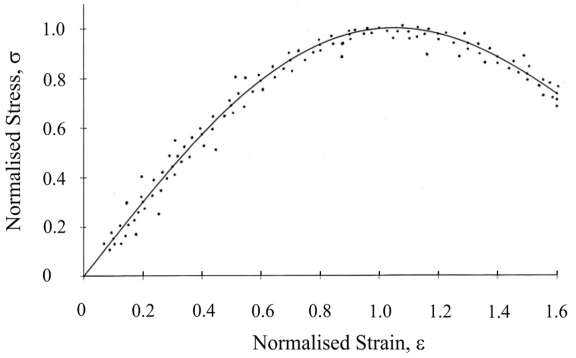

Fig. 9 Envelope stress-strain curve ($\theta = 45^{o}$)

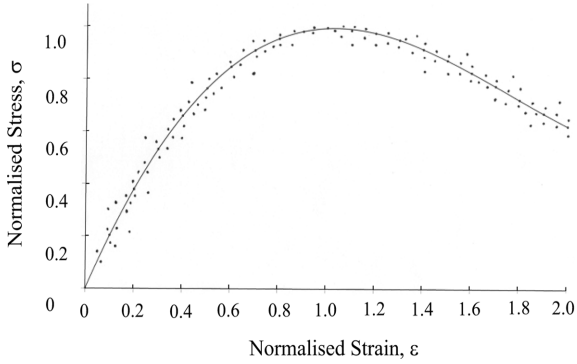

Fig. 10 Envelope stress-strain curve ($\theta = 67.5^{o}$)

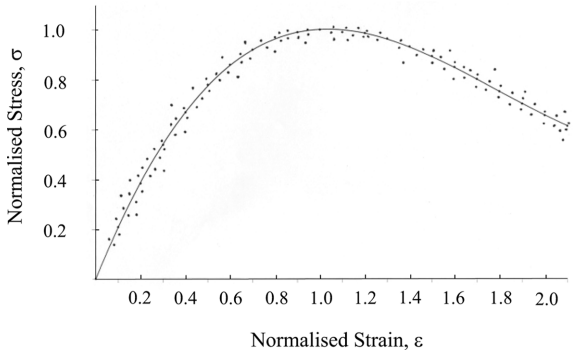

Fig. 11 Envelope stress-strain curve ($\theta = 90^{o}$)

to bed joints was found to be 1.15 based on the present study, compared to a ratio of 1.17 for calcium silicate bricks investigated by Milad and Sinha (2000) and Senthivel and Sinha (2003). However the ratio for similar bricks investigated by Singh and Sinha (2004a) was found to be 1.03, which is 10 percent lower than the ratio observed in the present investigation.

Additionally, a similar envelope of stress-strain curves was also obtained for specimen loaded at 0^{o} and 90^{o} to bed joints. Singh and Sinha (2004a) also observed an ultimate normalised strain of 1.3

for specimens loaded at 0° and 90° to bed joints, whereas in present study, the ultimate normalised strains were 1.9 and 2.1 for specimens loaded at 0° and 90° to bed joints, respectively. Other investigators (Powell and Hodgkinson 1976) have also observed high ultimate normalised strains up to 2.0 for different types of brickwork.

3.2.2 Common point curves

The cyclic loading tests in test Types II and III exhibited a locus of common points at the intersection of the reloading curve of any cycle and the unloading curve of the previous cycle. The common points obtained from test Types II and III are plotted in Figs. 12 to 16, for all five cases of loading. The stress coordinate is normalised with respect to the failure or peak stress, σ_m, of each specimen and the strain coordinate is normalised with respect to ε_m, the axial strain corresponding to σ_m.

3.2.3 Stability point curve

The cyclic loading test in test Type III exhibited a locus of stability points. The stability points obtained from test Type III have been plotted in Figs. 17 to 21, for all five cases of loading. The stress coordinate is normalised with respect to the failure stress, σ_m, of each specimen and the strain coordinate is normalised with respect to ε_m, the axial strain corresponding to σ_m.

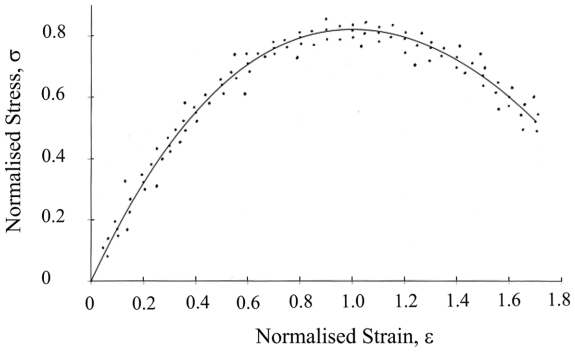

Fig. 12 Common point stress-strain curve ($\theta = 0^o$)

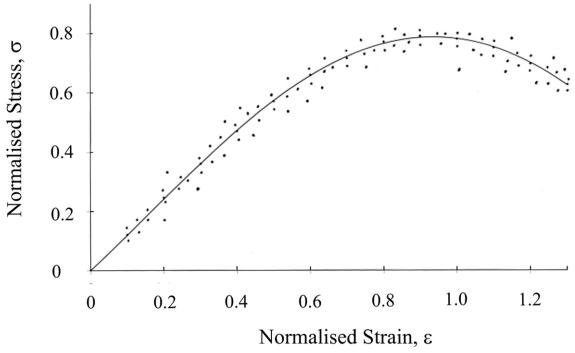

Fig. 13 Common point stress-strain curve ($\theta = 22.5^o$)

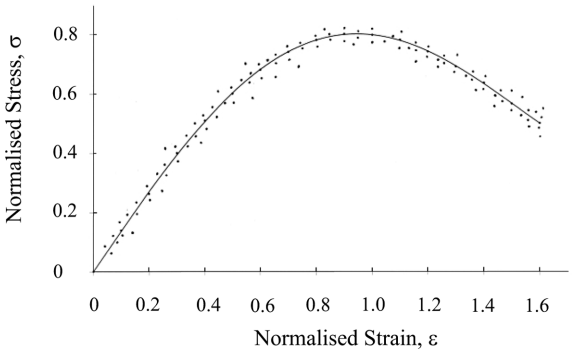

Fig. 14 Common point stress-strain curve ($\theta = 45^o$)

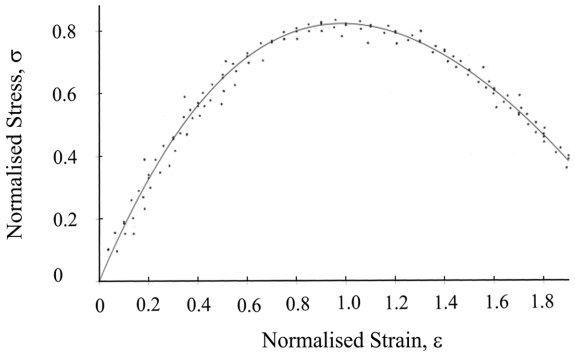

Fig. 15 Common point stress-strain curve ($\theta = 67.5^o$)

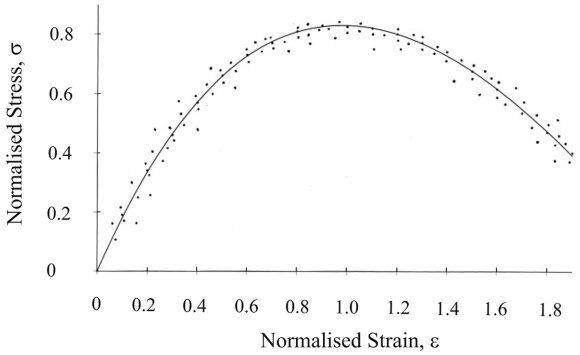

Fig. 16 Common point stress-strain curve ($\theta = 90^{o}$)

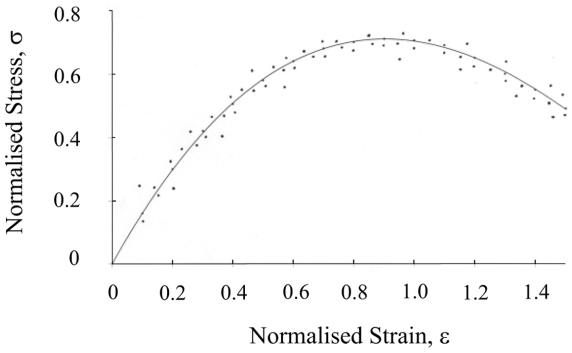

Fig. 17 Stability point stress-strain curve ($\theta = 0^{o}$)

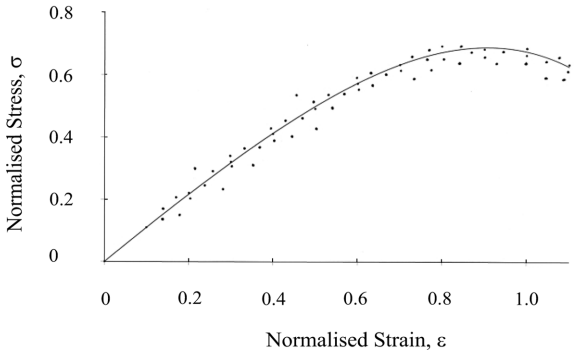

Fig. 18 Stability point stress-strain curve ($\theta = 22.5^{o}$)

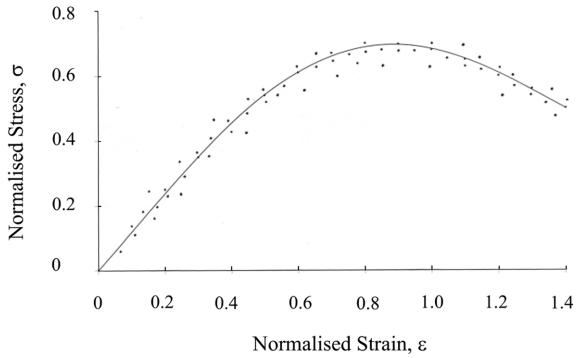

Fig. 19 Stability point stress-strain curve ($\theta = 45^{o}$)

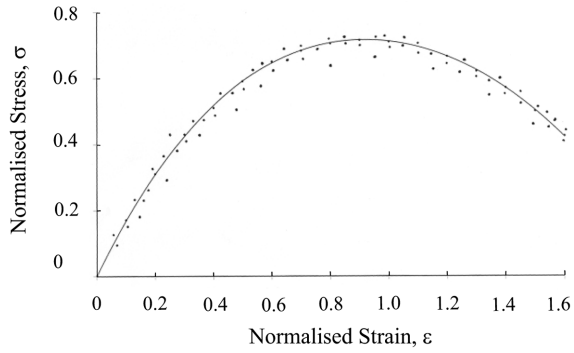

Fig. 20 Stability point stress-strain curve ($\theta = 67.5^{o}$)

3.2.4 Analytical curves

Based on experimental data a polynomial formulation was proposed for envelope, common point and stability point curves. The general form of the expression is,

$$\sigma = a\varepsilon^4 + b\varepsilon^3 + c\varepsilon^2 + d\varepsilon$$

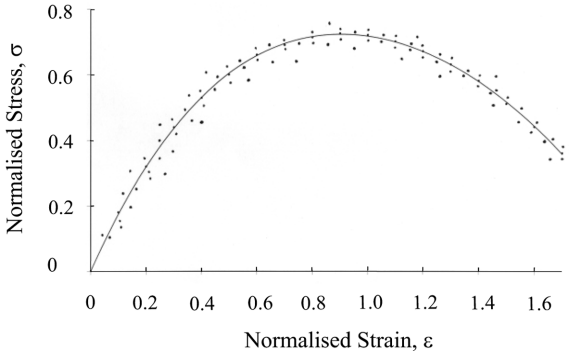

Fig. 21 Stability point stress-strain curve ($\theta = 90^o$)

Table 3 Values of a, b, c, d and i_c for envelope, common point and stability point curves

Stress-strain curve	Load case with respect to bed joint orientation, θ	Equation parameters				Correlation coefficient, (i_c)
		a	b	c	d	
Envelope curve	0°	0.0762	−0.0863	−0.9897	1.9975	0.9570
	22.5°	0.3247	−1.3353	0.7965	1.2115	0.9840
	45°	0.2376	0.8587	0.1081	1.5109	0.9835
	67.5°	0.0255	0.1655	−1.3594	2.1668	0.9515
	90°	−0.001	0.2878	−1.5289	2.2432	0.9423
Common point curve	0°	−0.0481	0.3022	−1.2808	1.8479	0.9415
	22.5°	0.2774	−1.1277	0.4788	1.1523	0.9730
	45°	0.2736	−0.8482	−0.0211	1.3934	0.9813
	67.5°	−0.0256	0.2697	−1.3090	1.8901	0.9641
	90°	−0.0367	0.3264	−1.4019	1.9427	0.9630
Stability point curve	0°	−0.0154	0.2179	−1.2286	1.7291	0.9527
	22.5°	−0.2591	−0.0087	−0.1796	1.1199	0.9710
	45°	0.4531	−1.3316	0.4032	1.1581	0.9663
	67.5°	−0.1109	0.5205	−1.5272	1.8295	0.9677
	90°	−0.1116	0.5739	−1.6497	1.9039	0.9511

where σ is normalised stress ratio σ_a/σ_m and ε is the normalised strain ratio $\varepsilon_a/\varepsilon_m$. By assigning suitable values of a, b, c and d, the equation is used to obtain the envelope, common point and stability point curves for interlocking grouted stabilised mud-flyash brick masonry. Table 3 gives the values of a, b, c and d for different load cases. The analytical curves for envelope points, common points and stability points for all load cases are plotted in Figs. 22 to 24. Based on these figures, the following observations are noted:

1. The degree of an fit of an analytical curve with the corresponding experimental data is indicated by the coefficient of variation, i_c, which is given in Table 3. It can be observed that the values of i_c range from 0.94 to 0.984. This implies a reasonable degree of fit between the analytical curves and the test data.

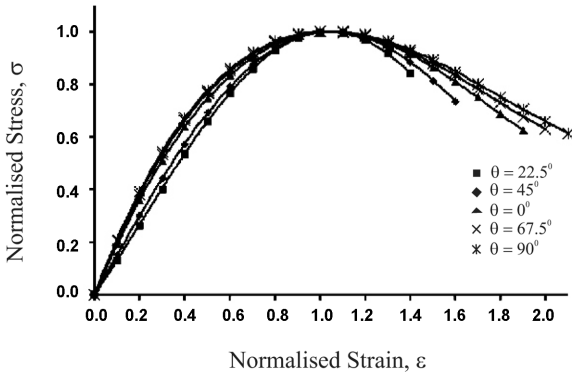

Fig. 22 Analytical envelope stress-strain curves

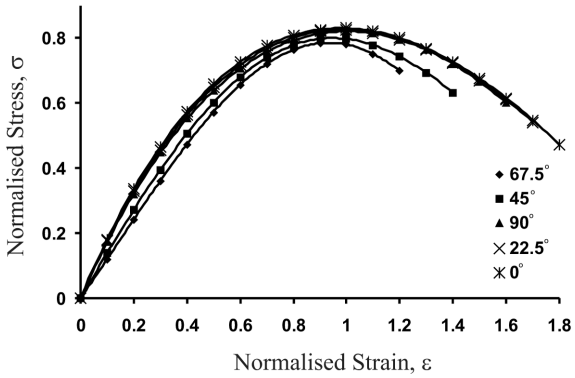

Fig. 23 Analytical common point stress-strain curves

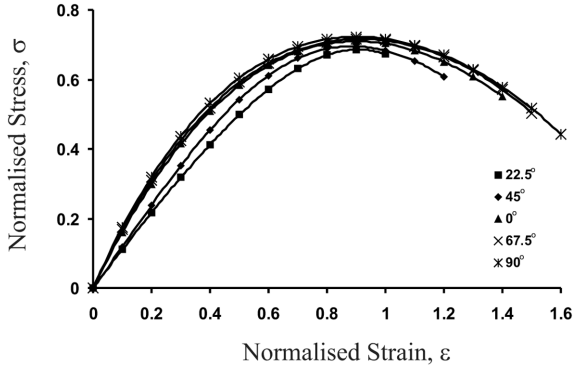

Fig. 24 Analytical stability point stress-strain curves

2. The non-dimensionalised envelope curves are shown in Fig. 22. The curves coincide approximately for specimens loaded at 0°, 67.5° and 90° to the bed joints up to peak stress ratio. Thereafter a decrease in stress ratio was observed beyond the peak stress ratio for specimens loaded at 67.5° and 0° to the bed joints in comparison to specimens loaded at 90° to the bed joints. Lower stress ratios with respect to other load cases were observed for specimens loaded at 45° and 22.5° to the bed joints.
3. The non-dimensionalised common point curves are shown in Fig. 23. The maximum stress ratio was observed for specimens loaded perpendicular to bed joints. A slight decrease in stress ratio was observed for specimens loaded at 67.5° and 0° in comparison to specimens loaded perpendicular to bed joints. The lower stress ratio exhibited for the specimens loaded at 45° to bed joints and stress ratio was lowest for the specimens loaded at 22.5° to the bed joints. This is because most of the specimens loaded at 22.5° and 45° to the bed joints were failed due to failure of joints.
4. The non-dimensional stability point curves are shown in Fig. 24. The same observations, as observed from common point curves are also observed from stability point curves. Maximum stress ratio was observed for specimens loaded at 90° to bed joints and lowest stress ratio was observed for specimens loaded at 22.5° to the bed joints.

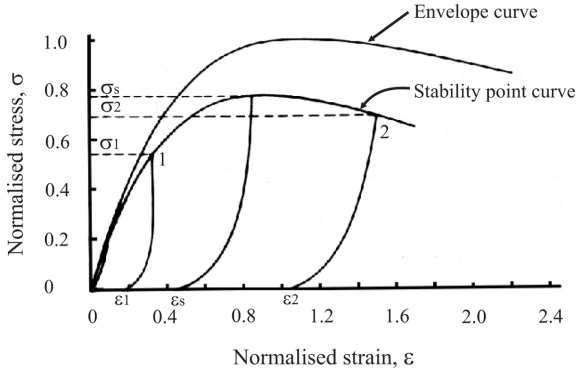

Fig. 25 Permissible stress level

5. The non-dimensional envelope curves for different load cases as shown in Fig. 22 have been found to compare well with the envelope curves obtained by Senthivel and Sinha (2003), for calcium silicate bricks.
6. The common point and stability point curves as shown in Fig. 23 and Fig. 24 are similar to those obtained by Senthivel and Sinha (2003), for the specimens loaded at 0°, 67.5° and 90° to bed joints.

3.3 Permissible stress level

The stability point curve may be used to define the permissible stress level, where reduction in stress due to the effect of repeated loading has to be considered. Stresses beyond the common point level produce plastic strain, while stresses below the common point level produce reduced plastic strain.

Load cycles with peak coinciding with the stability point curve does not produce additional plastic strain. If the peaks of the load cycles exceed the stability point limit ($\sigma > \sigma_s$) (Fig. 25), then the continuous cycling will cause an accumulation of plastic strain which eventually lead to failure. In case of the peak of cyclic stress, $\sigma < \sigma_s$, then continuous cycling will result in accumulation of plastic strain until if coincides with the stability point curve at point 1 (Fig. 25). Further cycling will follow the same path and plastic strain stablises at ε_1. The level of plastic strain in the material is, therefore, considered to be a prime factor in determining the permissible stress level. If the level of plastic strain ε_1 in the material is found to be less than plastic strain ε_s, corresponding to peak stress σ_s of the stability point curve, then σ_s can be considered as maximum permissible stress level. On the other hand, if the level of plastic strain ε_2 is more than the plastic strain ε_s than the corresponding stability point stress σ_2 can be regarded as the permissible stress level.

4. Conclusions

The results obtained from the investigation of the behaviour of interlocking grouted stabilised mud-flyash brick masonry under uniaxial cyclic compressive loading can be summarised as follows:

1. The peak value of the stress-strain curve under cyclic loading coincided approximately with that

of the envelope curve under monotonic loading. It is because the unloading is done when peak of the loading curve coincides with the envelope curve.

2. The stress-strain history possesses a locus of common and stability points. The stability point curve may be used to define the permissible stress level, when reduction in strength due to effect of repeated loading has to be considered.
3. The stress-strain envelope, common point and stability point curves can be represented by a mathematical polynomial formulation. The coefficient of variation of these equations with corresponding test data ranges from 0.94 to 0.984, which is indication of good agreement.
4. The load carrying capacity of interlocking grouted stabilised mud-flyash brick masonry system is 62 percent of its unit strength for panels loaded perpendicular to bed joints, whereas the ultimate strength of conventional masonry systems varies from 30 to 40 percent of the unit strength. Therefore, the brick masonry made with interlocking bricks is more efficient, having almost twice the load carrying capacity, then the conventional brick masonry.
5. Failure in compression occurred by splitting in bed joints for panels loaded at 0^o to the bed joints, whereas for panels loaded at 22.5^o, 45^o, 67.5^o and 90^o to bed joints, failure was characterized by a combined failure in brick units and joints.
6. The common point and stability point curves for panels loaded at 22.5^o and 45^o to the bed joints have been investigated in this study. However, the common point and stability point curves for panels loaded at 22.5^o and 45^o to the bed joints are not available in literature. But, such investigations were attempted by Senthivel and Sinha (2003) on conventional brick masonry but they could not achieved the common point and stability point curve due to failure of joints at early stage of loading. Other researchers such as Dhanasekar *et al.* (1985), Page (1981), Samarasinghe and Hendry (1980) have conducted tests on brickwork for different bed joint orientations but their findings were restricted to monotonic loading.

References

Abrams, D., Noland, J. and Atkinson, R. (1985), "Response of clay unit masonry to repeated compressive forces", *Proc. 7th Int. Brick. Masonry Conf.*, Melbourne, 565-576.

Chen, S.W.J., Hidalgo, P.A., Mayes, R.L., Clough, R.W. and McNiven, H.D. (1978), "Cyclic loading test of masonry single piers, volume 2 - Height to width ratio 1", EERC Rep. No. 78/28, Envir. Engrs. Res. Council, University of California, Berkley, California.

Choubey, U.B. and Sinha, S.N. (1991), "Cyclic compressive loading response of brick masonry", *J. Masonry Int.*, **4**(3), 94-98.

Choubey, U.B. (1992), "Cyclic stress-strain in stretcher bond", *Proc. of the fourth International Seminar on Structural Masonry for Developing Countries* (Madras), 70-80.

Dhanasekar, M., Kleeman, P.W. and Page, A.W. (1985), "The failure of brick masonry under biaxial stresses", *Proc. Inst. of Civil Engineers*, Part 2, **79**, 295-313.

Drysdale, R.G. and Guo, P. (1995), "Strength characteristic of interlocking dry-stacked concrete block masonry", *Proc. of the Seventh Canadian Masonry Symposium*, Hamilton, Ontario, 160-170.

Karsan, J.K. and Jersa, J.O. (1969), "Behaviour of concrete under compressive loading", *J. Street Div.*, ASCE, **95**(12), 2543-2563.

Macchi, G. (1985), "Behaviour of masonry under cyclic actions and seismic design", *Proc. Int. Brick Masonry Conf.*, LI-XXIV.

Milad, M.A. and Sinha, S.N. (2000), "Stress-strain characteristics of brick masonry under uniaxial loading", *J. Struct. Eng.*, ASCE, **125**(6), 600-604.

Naraine, K. and Sinha, S.N. (1989), "Behaviour of brick masonry under cyclic compressive loading", *J. Struct. Eng.*, ASCE, **115**(6), 600-604.
Page, A.W. (1981), "The biaxial compressive strength of brick masonry", *Proc. Inst. of Civil Engineers*, Part 2, **71**, 893-906.
Powell, B. and Hodgkinson, H.R. (1976), "The determination of stress-strain relationship of brickwork", *Proc. 4th Int. Brick Masonry Conf.*, Brugge, 2.a.5.1-2.a.5.6.
Reddy, B.V.V. (1991), "Studies on static soil compaction and compacted soil-cement blocks for walls", Ph.D. Thesis, Dept. of Civil Engineering, Indian Institute of Science, Bangalore, India.
Reddy, B.V.V. and Jagdish, K.S. (1995), "Influence of soil composition on strength and durability of soil cement blocks", *The Indian Concrete Journal*, **69**(9).
Samarasinghe, W. and Hendry, A.W. (1980), "Strength of brickwork under biaxial stresses", *7th Int. Symp. on Load Bearing Brickwork.*
Senthivel, R. and Sinha, S.N. (2003), "Energy dissipation response of brick masonry under cyclic compressive loading", *Struct. Eng. Mech.*, **16**(4), 405-422.
Singh, B.K. and Sinha, S.N. (2004a), "Stress-strain curves for interlocking grouted stabilised mud brick masonry in cyclic uniaxial compressive loading", *The Third Int. Conf. on Advances in Structural Engineering and Mechanics*, Seoul, Korea, 2278-2293.
Singh, B.K. and Sinha, S.N. (2004b), "Deformation characteristics of interlocking grouted mud block masonry", *7th Australian Masonry Conf.,* New Castle, New South Wales, Australia, 437-445.
Steadman, M., Drysdale, R.G. and Khattab, M.M. (1995), "Influence of block geometry and grout type on compressive strength of block masonry", *Proc. of the Seventh Canadian Masonry Symposium*, Hamilton, Ontario, 1116-1127.
Thomas, F.G. (1953), "The Strength of Brickwork", *Struct. Eng.*, **31**, 35-46.
Walker, P. (1995), "Strength, durability testing of earth blocks", *Cement and Concrete Composites*, **17**(4), 301-310.
Walker, P. (2000), "Strength and durability testing of earth blocks", *6th Int. Deminar on Structural Masonry for Developing Countries*. 11-13, Bangalore, India.
Worthing, G.W., Samarasinghe, W. and Lawrence, S.J. (1992), "Pressed earth blocks in Australia", *Proc. of Fourth Int. Seminar on Structural Masonry for Developing Countries* (Madras), 211-216.

Notation

a, b, c and d	: Equation parameter
i_c	: Coefficient of variation
ε	: Non-dimensional axial strain
ε_a	: Axial strain at any point 'a'
ε_m	: Axial strain at peak stress
ε_s	: Non-dimensional axial strain at peak of stability point stress
σ	: Non-dimensional axial stress
σ_a	: Axial stress at any point 'a'
σ_m	: Failure (peak) stress
σ_s	: Non-dimensional axial stress at the peak of stability point curve
θ	: Angle between loading direction and bed joints